Right atrial function by speckle tracking echocardiography in atrial septal defect: prediction of atrial fibrillation

Antonio Vitarelli, MD, FACC, Enrico Mangieri, MD, Carlo Gaudio, MD, Gaetano Tanzilli, MD, Fabio Miraldi, MD, Lidia Capotosto, MD. –

Cardiac Dept., Sapienza University, Rome, Italy

Word count: 2571 (including figure legends and excluding references)

Disclosures: We have no conflicts to disclose.

Address for correspondence:
Antonio Vitarelli, M.D.
Via Lima 35
00198 Rome, Italy
telephone number: 39/6/85301427,
FAX number: 39/6/8841926,
E-mail: vitar@tiscali.it
cardiodiagnostica@gmail.com

This article has been accepted for publication and undergone full peer review but has not been through the copyediting, typesetting, pagination and proofreading process, which may lead to differences between this version and the Version of Record. Please cite this article as doi: 10.1002/clc.23051

Condensed abstract

Purpose. To examine right atrial(RA) function by two-dimensional(2DSTE) and three-dimensional speckle-tracking-echocardiography(3DSTE) in patients with atrial septal defect(ASD) before and after implantation of atrial devices.

Methods. Seventy-three ASD patients after occluder insertion, 73 controls, and 17 patients who developed paroxysmal atrial fibrillation(PAF) were studied. RA peak-strain(PS), time-to-peak-strain(TPS), and expansion-index(EI) were determined.

Results. RA-PS and RA-EI(pre-closure values) were reduced in ASD patients. ROC curves for 3D-RA-EI, RA-PS, and RA-TPS(pre-closure values) showed high discriminative values(0.76-0.85) in predicting PAF.

Conclusions. In ASD-device patients speckle-tracking-echocardiography reveals pre-existent RA dysfunction with higher association with PAF compared to both the size of devices and left atrial indices.

Abstract

Purpose. The purpose of this study was to examine right atrial (RA) function by two-dimensional (2DSTE) and three-dimensional (3DSTE) speckle-tracking echocardiography in patients with atrial septal defect (ASD) who had implantation of septal occluders and developed paroxysmal atrial fibrillation (PAF).

Methods. Seventy-three patients with hemodynamically significant secundum ASD were prospectively studied and followed up for six months after occluder insertion and compared with a normal age-matched group(n=73). A subgroup of 17 patients who developed PAF after device implantation was also studied. RA peak global longitudinal strain (PS) was determined using 2DSTE. Standard deviations(SDs) of times to peak strain (TPS) were calculated as indices of dyssynchrony. RA volumes, emptying fraction (EF), and expansion index (EI) were determined using 3DSTE.

Results. RA PS, EF, and EI (pre-closure values) were reduced in patients with atrial devices compared with controls, and further reductions were observed in patients with PAF. Pre-closure 3D-RA-EI (p=0.009) and RA-TPS (p=0.023) were independent predictors of PAF by multivariate analysis after adjustment for age and left atrial dysfunction. The areas under the ROC-curve(AUC) for 3D-RA-EI, RA-PS, RA-TPS (pre-closure values) showed high discriminative values(from 0.76 to 0.85) in predicting PAF. By combining 3D-RA-EI and RA-TPS, the AUC increased to 0.90.

Conclusions. Two-dimensional and three-dimensional speckle tracking echocardiography was clinically helpful in ASD patients in revealing right atrial dilatation and dysfunction pre-existent to device closure and associated with PAF development. RA parameters had a higher association with PAF compared to both the size of the implanted device and left atrial indices.

Key words: right atrial function, atrial septal defect, echocardiography, speckle tracking echocardiography, atrial fibrillation.

Introduction.

Most antiarrhythmic interventional therapies for atrial fibrillation(AF) have been developed with special focus on the treatment of left-sided valvular disease and enlarged left atrium(1) but few studies have assessed AF associated with congenital heart disease and dilated right atrium(2). The transcatheter closure of atrial septal defect(ASD) has been described as a safe technique in patients with suitable anatomy(3,4) but it was hypothesized(5) that the occluder implantation could favor development of paroxysmal atrial fibrillation(PAF). It was also shown that biatrial volumes and function are abnormal in patients with PAF in the absence or in the presence of congenital atrial lesions (6-8) but studies focused on right atrial(RA) function are scanty (9,10). Thus we aimed to evaluate specifically RA function using two-dimensional and three-dimensional speckle tracking echocardiography in ASD patients who underwent occluders implantation and developed PAF in comparison with patients with atrial devices and normal sinus rhythm and a group of normal controls.

Methods.

Population. Seventy-three patients with hemodynamically significant ostium secundum ASD (aged 17-48 years) were included in the study and followed up for six months after occluder insertion. Patients with concomitant congenital heart disease, comorbidities, or pre-procedural AF were excluded from the study. PAF was diagnosed by documenting both sinus rhythm and AF on bedside ecg-monitoring or 2-8 day Holter-monitoring. All patients were in sinus rhythm at the time of echocardiographic examination. Seventy-three age- and sex-matched healthy subjects without cardiovascular disease chosen from the hospital staff and their relatives as part of check-up programs were recruited as controls.

Standard Echocardiography. Patients were examined with transthoracic echocardiography with a GE Vivid-E9 ultrasound scanner(GE Vingmed Ultrasound AS, Horten, Norway). Cardiac chambers were measured using to established criteria(11). Right atrial(RA) area was determined just before tricuspid valve opening from the apical four-chamber view, and RA maximal and

minimal volumes were also determined from the same views. Right ventricular systolic pressure was obtained using standard Doppler practices(11). The tricuspid E to E' ratio(E/E') was measured at the lateral corner of the tricuspid annulus in apical views and used as index for RA pressure.

Speckle tracking echocardiography. RA speckle tracking analysis was obtained in a transthoracic apical four-chamber view optimized for RA. RA STE curves were obtained using ECG R-wave as a reference point(12,13). RA peak global longitudinal strain at the end of the reservoir phase during ventricular systole (PS, peak strain) and strain in the atrial contractile phase during late ventricular diastole (ACS, atrial contraction strain) were measured by averaging the values of the six RA segments(Figure 1). RA dyssynchrony was quantified as the standard deviation of the time to peak strain using RA six-segment model in apical four-chamber views as previously reported for the LA(11). Time-to-peak strain(TPS) was computed as the standard deviation of the time to maximal positive deformation of each curve(Figure 1).

RA three-dimensional datasets were acquired in apical windows by aligning in such a way that the entire RV and RA were included. RA long-axis and short-axis views were obtained (Figure 1) and analyzed on a separate software workstation(EchoPAC BT13, 4D Auto LVQ, GE Vingmed Ultrasound, Horten, Norway). Volumetric curves were determined(14-16). RA volumes were defined as follows. RA maximal volume(Vmax)= volume at LV end-systole, the time at which atrial volume was largest just before mitral valve opening. RA minimal volume(Vmin)= volume at LV end-diastole, the time at which atrial volume is at its nadir before mitral valve closure. RA volume before atrial contraction(VpreA)= volume at LV early diastole, at the onset of P-wave on ECG (the last frame before mitral valve reopening). RA total emptying fraction(RA-EF)= [(RA-Vmax – RA-Vmin)/RA-Vmax] x 100. RA expansion index(RA-EI)= [(RA-Vmax – RA-Vmin)/RA-Vmin] x 100.

Occluder insertion. ASD size and morphology were determined by transesophageal echocardiography (TEE). Closure was achieved in all patients using Amplatzer septal occluder and Figulla Occlutech devices with a median size of 22 mm(range, 18-36 mm). The mean

estimated ASD size on TEE was 15.1±3.6 mm(range, 9-27 mm). The occluder was inserted under fluoroscopic and TEE guidance. Patients were discharged from the hospital after post-interventional transthoracic echocardiography.

Statistics. Categorical variables are presented as numbers and percentages and continuous data are expressed as mean ± SD. Differences among three or more groups were determined using one-way analysis of variance with post hoc comparisons by Bonferroni test. Differences were considered statistically significant when the p value was <0.05. Receiver operating characteristic (ROC) curves were used to determine diagnostic accuracy for PAF prediction. The optimal cut-off values of echo parameters were derived from ROC analysis by maximizing the sum of the sensitivity and specificity. The intra-observer and inter-observer variabilities were determined as the absolute difference between each observer's value divided by the mean of both measurements and expressed as a percentage (coefficient of variation). Intra-class correlation coefficients were also obtained with good agreement defined as having a coefficient >0.80.

Results.

Overall feasibility of RA two-dimensional speckle tracking echocardiography was 89% and overall feasibility of three-dimensional speckle tracking echocardiography for volumetric RA analysis was 92%. Ten patients were excluded in the presence of more than two uninterpretable segments (n=8 both 2DSTE and 3DSTE, n=2 only 2DSTE). In six patients with relatively vigorous tricuspid annular motion, speckle tracking of the RA free wall segment adjacent to the tricuspid valve was adversely affected and this segment was excluded from analysis.

Coefficients of variation ranged for 2D measures from 3% to 12%, and for 3D measures from 3% to 10%. Intraclass coefficients ranged for 2D measures from 0.80 to 0.88, and for 3D measures from 0.83 to 93.

PAF overall incidence after 6 months follow-up was 23%(17/73 patients). Two patients presented with pulmonary embolism and ischemic stroke, respectively, following AF during antiplatelet therapy. Baseline characteristics and echocardiographic findings of the patients are

presented in Table 1. ASD patients with PAF tended to be older than patients with normal sinus rhythm (NSR) but the difference did not reach statistical significance. No differences were found between groups in body surface area, body mass index, systemic blood pressure, and heart rate. RA PS, EF, and EI(both pre-closure and post-closure values) were reduced in patients with septal occluders compared with the control group. 3DSTE-derived RA volumes and TPS were larger in PAF patients (Table 1). A moderate positive relationship was observed between 2D and 3DSTE techniques for RA-Vmax (r=0.62,p=0.014) and RA-Vmin (r=0.58,p=0.029). Five patients with ASD had atrial septal aneurysms and four patients had mild mitral regurgitation from mild mitral valve prolapse. There was a moderately significant increase in left atrial dyssynchrony (LA-TPS: 96.3±29.6msec vs 84.2±23.6msec, $p<0.05$) and a moderately significant decrease in 3D left atrial expansion index (131.6 ±39.7% vs 157.2 ±40.5, $p<0.05$) compared to controls.

The time course of pre-closure RA volumetric and functional parameters on six-months follow-up after occlude implantation (Table 2) showed that pre-existent atrial dysfunction persisted during the 6-months follow-up in spite of partial reduction of atrial volumes. Septal strain was lower in patients with device compared to lateral wall strain but did not influence significantly the post-closure global longitudinal strain value.

Devices diameters ranged from 18 to 36 mm. A weak correlation was found between device size and RA parameters with reduced 3D-RA-EI(r=-0.411,p=0.034) and increased RA-TPS(r=0.383,p=0.041).

Multivariate analysis (Table 3) showed that pre-closure 3D-RA-EI (r=-0.479, p=0.009) and RA-TPS (r=0.315, p=0.023) were independently associated with PAF after adjustment for covariates (age, left atrial expansion index, left atrial dyssynchrony index). In Figure 1 the areas under the ROC-curve(AUC) for 3D-RA-EI, RA-PS, RA-TPS (pre-closure values) suggested high discriminative values(from 0.76 to 0.85) in predicting PAF. By combining 3D-RA-EI and RA-TPS, the AUC increased to 0.90.

Discussion.

We have shown that 1) in ASD patients who underwent successful device closure pre-existent right atrial dilatation and dyssynchrony had a significant association with PAF independently of left atrial dysfunction; 2) right atrial parameters had a higher association with PAF compared to both the size of the implanted device and left atrial indices; 3) the combination of right atrial volumetric indices(expansion index) and deformation parameters(time to peak strain) provided stronger estimates of PAF risk compared to other RA indices.

Validation of 3DSTE atrial volumetry with cardiac magnetic resonance has been previously reported(16). Two-dimensional and 3DSTE methods showed a satisfactory correlation in the assessment of RA volumes, in spite of 3D better reproducibility indicated by a lower inter-observer difference and variability. RA expansion index, an expression of the RA minimal volume, strongly predicted atrial fibrillation. This suggests that minimal atrial size, which is related to instantaneous loading conditions more than maximal atrial volume (17,18) since in end-diastole the tricuspid valve is open, is more sensitive to slight pathologic changes due to fibrosis or remodeling.

The link between ASD and AF was previously reported (19,20) and RA catheter ablation was suggested in selected cases (21,22). RA stretch and dyssynchrony caused by left-to-right shunt promotes changes in atrial refractoriness and ionic currents(electrical remodeling), as well as tissue remodeling due to atrial fibrosis(structural remodeling), that generate a favorable substrate for AF initiation. RA and RV volumes are reduced following the septal occluder procedure, but some structural and electrical remodeling may persist.

In ASD patients the pathophysiological events related to PAF episodes were pre-existent RA overload and device insertion, thus we studied RA dyssynchrony by determining the time to peak strain in the reservoir phase(23) rather than during atrial contractile phase(1,24). RA pre-closure strain, dyssynchrony and volumetric parameters were significantly different compared to normal controls and associated with PAF. RA indices impairment persisted for up to 6 months after the occluder insertion. In ASD-device patients septal strain was lower than lateral wall strain but did not significantly affect the post-procedure global peak strain. Moreover, a weak relationship was

shown between the sizes of septal occluders, RA parameters and FA. These data indicate that pre-closure RA changes more than the sizes of septal occluders favor PAF development following ASD interventional procedures, in keeping with the findings that we reported in a mixed population with patent foramen ovale and atrial septal defect (8).

Patients had significant RA dilatation compared to controls. The parossistic atrial arrhythmia was associated with major changes in the right atrium rather than in the left atrium as it is typically observed in mitral valve disease. At a time when clinical atrial fibrillation becomes obvious, since RA and LA share muscular fibers, histological changes should not be limited to the right atrium and may not exactly match the clinically measured atrial enlargement degree (22). Prolonged arrhythmic history could induce alterations in the right atrial tissues and similarly in left atrial tissues. Once clinical atrial fibrillation is persistent, it is questionable whether only a right atrial therapeutic approach is as effective as expected, and in this particular stage the presence of atrial fibrillation should justify an additional electrophysiological investigation. However, this exceeds the purpose of the present study.

Clinical implications. We have previously shown (8) that in patients with patent foramen ovale and atrial septal defect bi-atrial dysfunction pre-existent to device implantation was associated with PAF development. In the present study we found that in ASD patients right atrial dilatation and dyssynchrony was associated with PAF independently of left atrial dysfunction and with higher significance than left atrial parameters. The combined assessment of 3D RA volumetric(EI) indices and RA dyssynchrony(TPS) appeared the best plan for AF prediction and more sensitive than conventional volumetric atrial indices. Since it has been shown that the severity of RA histopathologic change can be independent of the degree of RA volume dilatation (25), the two indices are complementary to each other.

Our results support elective closure of significant ASD once the diagnosis is made as a preventative strategy against AF. Moreover, these findings corroborate the concept that the right atrium should no longer be a forgotten part of the heart in atrial fibrillation, and ablation only on the

left side would not be the choice in the field of congenital heart disease since most of responsible scars are present on the right side from the beginning (22,26,27). Furthermore, in the presence of persistent right atrial dilatation and dysfunction serial 12-lead ECGs and Holter monitoring should be recommended to detect AF as early as possible, and anticoagulation may be required as an adjunct to prophylactic antiarrhythmic and antifibrotic therapy or in place of antiplatelet therapy.

Limitations. A technical limitation is that the low temporal resolution of 3DSTE(16) affects the ability to track anatomic details frame by frame and requires multibeat(six beats) acquisitions. Further research leading to improvements in both hardware and software is required to assess the feasibility of 3DSTE and the relative importance of current limitations, such as the low frame rates and suboptimal image quality.

Secondly, patients with co-morbidities were ruled out, and this may reduce the generalization of the results of the present study. Furthermore, this was a single center protocol with a relatively small number of patients, thus a larger study is required to confirm our findings.

Conclusions. Two-dimensional and three-dimensional speckle tracking echocardiography, despite technical limitations, appeared as a sensitive and helpful method in ASD patients in revealing right atrial dilatation and dysfunction which was pre-existent to device closure and had a higher association with PAF compared to left atrial indices.

References

1. Sarvari SI, Haugaa KH, Stokke TM, Ansari HZ, Leren IS, Hegbom F, Smiseth OA, Edvardsen T. Strain echocardiographic assessment of left atrial function predicts recurrence of atrial fibrillation. Eur Heart J Cardiovasc Imaging 2016;17:660-667.
2. Nyboe C, Olsen MS, Nielsen-Kudsk JE, Hjortdal VE. Atrial fibrillation and stroke in adult patients with atrial septal defect and the long-term effect of closure. Heart 2015;101:706-711.
3. Silvestry FE, Cohen MS, Armsby LB, Burkule NJ, Fleishman CE, Hijazi ZM, Lang RM, Rome JJ, Wang Y; American Society of Echocardiography; Society for Cardiac Angiography and Interventions. Guidelines for the echocardiographic assessment of atrial septal defect and patent foramen ovale. JAmSocEchocardiogr 2015;28:910-958.

4. Vitarelli A, Sardella G, DiRoma A, Capotosto L, De Curtis G, D'Orazio S, Cicconetti P, Battaglia D, Caranci F, De Maio M, Bruno P, Vitarelli M, De Chiara S, D'Ascanio M. Assessment of right ventricular function by three-dimensional echocardiography and myocardial strain imaging in adult atrial septal defect before and after percutaneous closure. IntJCardiovascImaging 2012;28:1905-1916.
5. Johnson JN, Marquardt ML, Ackerman MJ, Asirvatham SJ, Reeder GS, Cabalka AK, Cetta F, Hagler DJ. Electrocardiographic changes and arrhythmias following percutaneous atrial septal defect and patent foramen ovale device closure. CathCardiovascInterv2011;78:254-261.
6. Akutsu Y, Kaneko K, Kodama Y, Suyama J, Li HL, Hamazaki Y, Tanno K, Gokan T, Kobayashi Y. Association between left and right atrial remodeling with atrial fibrillation recurrence after pulmonary vein catheter ablation in patients with paroxysmal atrial fibrillation: a pilot study. Circ Cardiovasc Imaging 2011;4:524-531.
7. Bai Y, Zhao Y, Li J, Zhang Y, Bai R, Du X, Dong JZ, He YH, Ma CS. Association of peak atrial longitudinal strain with atrial fibrillation recurrence in patients with chronic lung diseases following radiofrequency ablation. Intern Med J 2018 Feb 20. doi: 10.1111/imj.13768.
8. Vitarelli A, Gaudio C, Mangieri E, Capotosto L, Tanzilli G, Ricci S, Viceconte N, Placanica A, Placanica G, Ashurov R. Biatrial function before and after percutaneous closure of atrial septum in patients with and without paroxysmal atrial fibrillation: a two-dimensional and three-dimensional speckle tracking echocardiographic study. Ultrasound Med Biol 2018, 44:1198-1211.
9. Xie E, Yu R, Venkatesh BA, Bakhshi H, Heckber S, Soliman E, Bluemke D, Kawut S, Nazarian S, Lima J. Association of right atrial function with incident atrial fibrillation: the multi-ethnic study of atherosclerosis (MESA). J Am Coll Cardiol 2017;69(11):1570 (abstr). doi.org/10.1016/S0735-1097(17)34959-8.
10. Govindan M, Kiotsekoglou A, Saha SK, Camm AJ. Right atrial myocardial deformation by two-dimensional speckle tracking echocardiography predicts recurrence in paroxysmal atrial fibrillation. J Echocardiogr 2017;15:166-175.
11. Lang RM, Badano LP, Mor-Avi V, Afilalo J, Armstrong A, Ernande L, Flachskampf FA, Foster E, Goldstein SA, Kuznetsova T, Lancellotti P, Muraru D, Picard MH, Rietzschel ER, Rudski L, Spencer KT, Tsang W, Voigt JU. Recommendations for cardiac chamber quantification by echocardiography in adults. JAmSocEchocardiogr2015;28:1-39.
12. Hoit BD. Left atrial size and function: role in prognosis. JAmCollCardiol 2014;63:493-505.
13. Badano LP, Kolias TJ, Muraru D, Abraham TP, Aurigemma G, Edvardsen T, D'Hooge J, Donal E, Fraser AG, Marwick T, Mertens L, Popescu BA, Sengupta PP, Lancellotti P, Thomas JD, Voigt JU; EACVI Scientific Documents Committee. Standardization of left atrial, right ventricular, and right atrial deformation imaging using two-dimensional speckle tracking echocardiography: a consensus document of the EACVI/ASE/Industry Task Force to standardize deformation imaging. Eur Heart J Cardiovasc Imaging 2018 Mar 27. doi: 10.1093/ehjci/jey042.
14. Peluso D, Badano LP, Muraru D, Dal Bianco L, Cucchini U, Kocabay G, Kovàcs A, Casablanca S, Iliceto S. Right atrial size and function assessed with three-dimensional and speckle-tracking echocardiography in 200 healthy volunteers. EurHeartJCardiovascImaging 2013;14:1106-1114.

15. Teixeira R, Monteiro R, Garcia J, Baptista R, Ribeiro M, Cardim N, Gonçalves L. The relationship between tricuspid regurgitation severity and right atrial mechanics: a speckle tracking echocardiography study. IntJCardiovascImaging 2015;31:1125-1135.
16. Perez de Isla L, Feltes G, Moreno J, Martinez W, Saltijeral A, de Agustin JA, Gomez de Diego JJ, Marcos-Alberca P, Luaces M, Ferreiros J, Garcia Fernandez MA, Macaya C. Quantification of left atrial volumes using three-dimensional wall motion tracking echocardiographic technology: comparison with cardiac magnetic resonance. EurHeartJCardiovascImaging 2014;15:793-739.
17. Hsiao SH, Chiou KR. Left atrial expansion index predicts all-cause mortality and heart failure admissions in dyspnoea. Eur J Heart Fail 2013;15:1245-1252.
18. Riesenkampff E, Mengelkamp L, Mueller M, Kropf S, Abdul-Khaliq H, Sarikouch S, Beerbaum P, Hetzer R, Steendijk P, Berger F, Kuehne T. Integrated analysis of atrioventricular interactions in tetralogy of Fallot. Am J Physiol Heart Circ Physiol 2010;299:H364-371.
19. Contractor T, Mandapati R. Arrhythmias in patients with atrial defects. Card Electrophysiol Clin 2017;9(2):235-244.
20. Karunanithi Z, Nyboe C, Hjortdal VE. Long-term risk of atrial fibrillation and stroke in patients with atrial septal defect diagnosed in childhood. Am J Cardiol 2017;119:461-465.
21. Khairy P, Van Hare GF, Balaji S, Berul CI, Cecchin F, Cohen MI, Daniels CJ, Deal BJ, Dearani JA, Groot Nd, Dubin AM, Harris L, Janousek J, Kanter RJ, Karpawich PP, Perry JC, Seslar SP, Shah MJ, Silka MJ, Triedman JK, Walsh EP, Warnes CA. PACES/HRS Expert Consensus Statement on the Recognition and Management of Arrhythmias in Adult Congenital Heart Disease: developed in partnership between the Pediatric and Congenital Electrophysiology Society (PACES) and the Heart Rhythm Society (HRS). Endorsed by the governing bodies of PACES, HRS, the American College of Cardiology (ACC), the American Heart Association (AHA), the European Heart Rhythm Association (EHRA), the Canadian Heart Rhythm Society (CHRS), and the International Society for Adult Congenital Heart Disease (ISACHD). Can J Cardiol 2014;30:e1-e63.
22. Uemura H. Surgical aspects of atrial arrhythmia : Right atrial ablation and anti-arrhythmic surgery in congenital heart disease. Herzschrittmacherther Elektrophysiol 2016;27:137-142.
23. Degiovanni A, Bortnik M, Dell'Era G, Bolzani V, Occhetta E, Bellomo G, Marino P. Analysis of electrical and mechanical left atrial properties in patients with persistent atrial fibrillation. IntJCardiovascImaging 2013;29:71-78.
24. Loghin C, Karimzadehnajar K, Ekeruo IA, Mukerji SS, Memon NB, Kantharia BK. Outcome of pulmonary vein isolation ablation for paroxysmal atrial fibrillation: predictive role of left atrial mechanical dyssynchrony by speckle tracking echocardiography. JIntervCardElectrophysiol 2014;39:7-15.
25. Kwak JG, Seo JW, Oh SS, Lee SY, Ham EK, Kim WH, Kim SJ, Bae EJ, Lim C, Lee CH, Lee C. Histopathologic analysis of atrial tissue in patients with atrial fibrillation: comparison between patients with atrial septal defect and patients with mitral valvular heart disease. Cardiovasc Pathol 2014;23:185-192.
26. Burnett LA, Kocheril AG. Putative role of right atrial ablation in atrial fibrillation. J Atr Fibrillation 2014;6(6):1085.
27. Hayashi K, An Y, Nagashima M, Hiroshima K, Ohe M, Makihara Y, Yamashita K, Yamazato S, Fukunaga M, Sonoda K, Ando K, Goya M. Importance of nonpulmonary vein

foci in catheter ablation for paroxysmal atrial fibrillation. Heart Rhythm 2015;12:1918-1924.

Figure legends

Figure 1. Speckle-tracking volumetric and deformation right atrial parameters in ASD patients who underwent device implantation and predictive value of pre-closure RA indices for paroxysmal atrial fibrillation. **A**. Representative image of three-dimensional volumetric speckle tracking echocardiography. Broken line: time–right atrial volume curve(ml). RA=right atrium; Vmax=maximal volume at RV end-systole; Vmin=minimal volume at RV end-diastole; VpreA=volume before atrial contraction at RV early diastole. **B**. Representative image of two-dimensional speckle tracking echocardiography and RA dyssynchrony. PS= peak strain. The average of all 6 segments during 3 cardiac cycles was calculated. TPS= time to peak strain. The asterisk shows peak strain in different segments. The standard deviation of all 6 segments during 3 cardiac cycles was calculated.

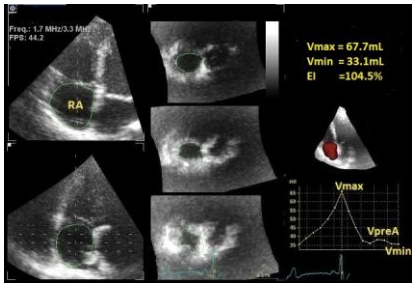

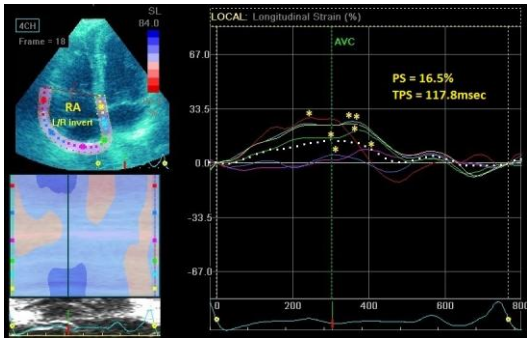

Figure 2. ROC curves comparing device size and pre-closure right atrial echocardiographic parameters for their accuracy to predict PAF.

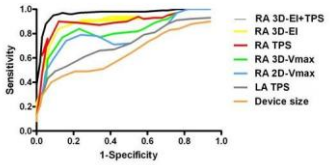

Variable	AUC	95% CI	Cut-off	Sensitivity	Specificity
Device size, mm	0.589	0.532-0.719	27	51	55
LA-TPS, msec	0.656	0.613-0.761	121	62	67
RA-2D-Vmax, ml/m^2	0.667	0.636-0.799	24	64	69
RA-TPS, msec	0.839	0.753-0.882	109	83	80
RA-3D-Vmax, ml/m^2	0.734	0.678-0.779	30	68	79
RA-3D-EI, %	0.851	0.781-0.889	117	85	83
RA 3D-EI +TPS	0.902	0.813-0.933	117, 109	90	85

Table 1. Baseline characteristics and echocardiographic parameters in controls, NSR patients and PAF patients

Variable	Controls (n=73)	ASD (n = 73)			p value
		NSR (n = 56)		PAF (n = 17)	
		Pre-closure	Post-closure	Pre-closure	
Age, yrs	43.3±3.2	42.9±3.6	42.9±3.6	44.7±3.4	NS
BSA, m^2	1.87±0.46	1.88±0.43	1.88±0.43	1.89±0.48	NS
BMI, kg/m^2	25.9±4.4	26.1±3.9	26.1±3.9	26.9±4.3	NS
HR, beats/m	72±14	71±12	72±15	74±13	NS
SBP, mmHg	123.8±21.9	124.2±23.4	125.6±23.9	126.9±22.8	NS
DBP, mmHg	71.9±12.3	71.2±14.1	72.4±13.7	72.8±13.2	NS
Smoking	18(25%)	13(23%)	13(23%)	4(24%)	NS
PASP, mmHg	25.6±3.6	30.9±3.8	29.8±3.4	31.5±3.9	0.05
2D-RA-AI, cm^2/m^2	8.4±2.6	10.2±2.5 *	10.1±2.2 *	10.5±2.4 *	0.05
2D-RA-Vmax, mL/m^2	23.2±3.3	24.8±3.4 *	24.2±3.2 *	25.4±3.1 *	0.05
2D-RA-Vmin, mL/m^2	10.2±1.9	12.6±2.3 *****	12.1±2.2 *****	12.7±2.5 *****	0.05
RA-PS, (%)	39.7±7.5	29.6±5.2 *	28.4±4.8 *	26.5±6.6 ***** ‡	0.001
RA-ACS, %	17.5±4.8	16.7±4.4	16.5±4.5	16.8±4.7	NS
RA-TPS, msec	78.6±21.9	105.4±24.8	109.1±23.6	114.8±22.7 † **§**	0.0005
RA stiffness, (T-E/E')/RA-PS	0.14±0.07	0.32±0.11 *	0.33±0.14 *	0.34±0.13	0.001
RA-PS-LW, %	38.4±7.7	36.6±7.2	36.1±7.1	36.7±6.8	0.001
3D-RA-Vmax index, ml/m^2	24.2±3.5	31.9±6.4 *	29.2±6.1 *	32.8±5.7	0.01
3D-RA-VpreA index, ml/m^2	14.4±2.8	15.4±3.2	15.2±3.1	15.5±3.3	NS
3D-RA-Vmin index, ml/m^2	10.3±2.1	12.8±3.2 ‡	12.1±2.4 ‡	13.4±2.7	0.001
3D-RA-EF, %	55.6±9.2	53.5±9.4 *	54.1±8.5 *	50.6±8.9	0.01
3D-RA-EI, %	148.7 ±32.8	110.2 ±27.4 ‡	114.9 ±26.2 ‡	99.3±25.4 † ‖	0.0001

3D= three-dimensional; 2D= two-dimensional; ACS= atrial contraction strain; AI= area index; BMI= body mass index; BSA= body surface area; DBP= diastolic blood pressure; E= inflow early diastolic velocity; E'= annular early diastolic velocity; EF= total emptying fraction (see text); EI= expansion index (see text); HR= heart rate; LW= lateral wall; NSR= patients with stable normal sinus rhythm within 6 months; PAF= patients who developed paroxysmal atrial fibrillation within 6 months after the 24hours post-procedure study; PASP= pulmonary arterial systolic pressure (echo); PS= peak global longitudinal strain (average); RA= right atrial; SBP= systolic blood pressure; T= tricuspid; TPS= time-to-peak strain (standard deviation); Vmax= maximal volume; Vmin= minimal volume; VpreA= volume before atrial contraction. Values are mean ± SD.

***** p<0.05 vs controls; † p<0.001 vs NSR; ‡ p<0.001 vs controls; **§** p<0.0005 vs controls; || p<0.0001 vs controls

Table 2. Temporal effects of STE right atrial parameters in controls (n=73) and ASD patients (n=73) during 6months follow-up (pre-closure, post 24 Hours, post 6 months)

Variable	ASD Pre-closure	ASD Post 24 Hours	ASD Post 6 months	Controls	p1	p2	p3	p4
RA-PS, (%)	29.6±5.2	28.4±4.8	30.8±4.7	38.1±7.4	NS	<0.05	<0.05	<0.05
RA-ACS, %	16.7±4.4	16.5±4.6	16.8±4.5	17.5±4.8	NS	NS	NS	NS
RA-TPS, msec	105.4±24.8	109.1±23.6	103.7±20.4	78.6±21.9	NS	<0.01	<0.01	<0.01
RA stiffness, (T-E/E')/RA-PS	0.32±0.11	0.33±0.14	0.30±0.17	0.14±0.07	NS	<0.05	<0.05	<0.05
RA-PS-SW, %	30.9±6.7	15.4±2.8	17.3±3.4	37.2±5.6	<0.01	<0.05	<0.01	<0.01
RA-PS-LW, %	36.6±7.2	36.1±7.1	36.9±4.8	38.4±7.7	NS	<0.05	<0.05	<0.05
3D-RA-Vmax, ml/m^2	31.9±6.4	29.2±6.1	27.6±5.7	24.2±3.5	<0.05	<0.01	<0.05	<0.05
3D-RA-VpreA, ml/m^2	15.4±3.2	15.2±3.1	15.1±3.5	14.4±2.8	NS	NS	NS	NS
3D-RA-Vmin, ml/m^2	12.8±3.2	12.1±2.4	11.7±2.8	10.3±2.1	<0.05	<0.01	<0.05	<0.05
3D-RA-EF, %	53.5±9.4	54.1±8.5	55.2±9.1	55.6±9.2	NS	<0.05	<0.05	NS
3D-RA-EI, %	110.2 ±27.4	114.9 ±26.2	119.2 ±31.9	148.7 ±32.8	NS	<0.01	<0.01	<0.01

3D= three-dimensional; ACS= atrial contraction strain; E= inflow early diastolic velocity; E'= annular early diastolic velocity; EF= total emptying fraction (see text); EI= expansion index (see text); LW= lateral wall; NS= not significant; PS= peak global longitudinal strain (average); RA= right atrial; SW= septal wall; T= tricuspid; TPS= time-to-peak strain (standard deviation); Vmax= maximal volume index; Vmin= minimal volume index; VpreA= volume before atrial contraction (index).
p1 = pre-closure vs. post 6 month; p2 = pre-closure vs. controls; p3 = post 24 hours vs. controls; p4 = post 6 month vs. controls.

Table 3. Multiple regression analysis showing pre-closure clinical and echocardiographic indices as independent predictors of PAF in ASD patients with atrial devices

	Univariate analysis		*Multivariate analysis **	
	r	p	r	p
Age	0.391	0.028		
BMI	0.319	0.059		
Smoking	0.238	0.077		
LVMI	0.387	0.047		
LA-TPS	0.391	0.045		
RA-PS	-0.417	0.024		
RA-TPS	0.599	0.008	0.315	0.023
2D-RA-Vmax	0.397	0.038		
2D-RA-Vmin	0.402	0.029		
3D-LA-Vmax	0.276	0.057		

3D-LA-EI	-0.348	0.041		
3D-RA-Vmax	0.477	0.031		
3D-RA-Vmin	0.686	0.017		
3D-RA-EI	-0.692	0.001	-0.479	0.009

3D= three-dimensional; 2D= two-dimensional; BMI= body mass index; EI= expansion index (see text); LVMI= left ventricular mass index; PS= peak strain (average); TPS= time-to-peak strain (standard deviation); Vmax= maximal volume index; Vmin= minimal volume index.
* Adjusted for age, LVMI, 3D-LA-Vmax, 3D-LA-EI, LA-PS, LA-TPS